Collective flow and energy loss with parton transport

I. Bouras[1], A. El[1], O. Fochler[1], F. Reining[1], J. Uphoff[1], C. Wesp[1], Z. Xu[1][2] and C. Greiner[1]

[1] *Institut für Theoretische Physik, Goethe Universität Frankfurt - Max-von-Laue-Strasse 1*
    D-60438 Frankfurt am Main, Germany
[2] *Frankfurt Institute for Advanced Studies - Ruth-Moufang-Strasse 1*
    D-60438 Frankfurt am Main, Germany

Summary. — Quenching of gluonic jets and heavy quark production in Au + Au collisions at RHIC can be understood within the pQCD-based (3+1)-dimensional parton transport model BAMPS including pQCD bremsstrahlung $2 \leftrightarrow 3$ processes. Furthermore, the development of conical structures induced by gluonic jets is investigated in a static box for the regimes of small and large dissipation.

PACS `25.75.-q` – Relativistic heavy-ion collisions.
PACS `24.10.Lx` – Monte Carlo simulations.
PACS `52.35.Tc` – Shock waves and discontinuities.
PACS `25.75.Cj` – heavy quark production in HIC.

1. – Introduction

The values of the elliptic flow parameter v_2 measured by the experiments at the Relativistic Heavy-Ion collider (RHIC) [1-3] suggest that in the evolving QCD fireball a fast local equilibration of quarks and gluon occurs at a very short time scale $\leq 1\,\mathrm{fm}/c$. This locally thermalized state of matter, the quark gluon plasma (QGP), behaves as a nearly perfect fluid, confirmed by viscous hydrodynamics [4,5] and microscopic transport theory [6,7]. The viscosity to entropy ratio coefficient η/s has to be rather small, possibly close to the conjectured lower bound $\eta/s = 1/4\pi$ from a correspondence between conformal field theory and string theory in an anti–de-Sitter space [8]. To achieve a rather small η/s value in a partonic gas, binary perturbative QCD (pQCD) processes require unphysical large cross-sections and thus inelastic radiative interactions [9] become important.

The phenomenon of jet-quenching has been another important discovery at RHIC [10]. Hadrons with high transverse momenta are suppressed in Au + Au collisions with respect to a scaled $p + p$ reference [11, 12]. This quenching of jets is commonly attributed to energy loss on the partonic level as the hard partons produced in initial interactions are bound to traverse the QGP created in the early stages of heavy-ion collisions (HIC).
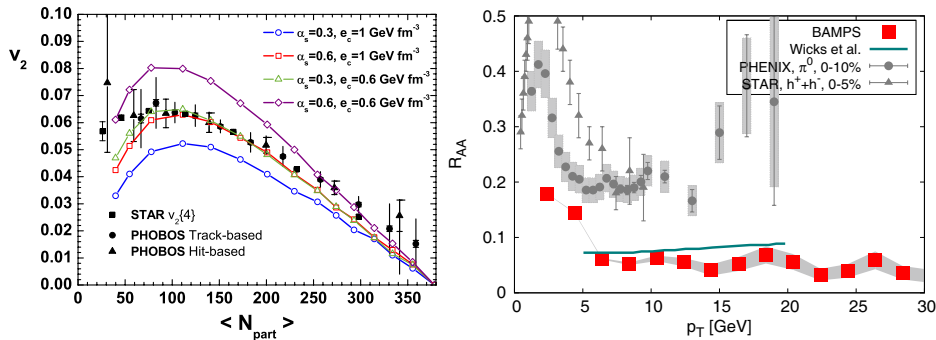
Fig. 1. – Left panel: elliptic flow v_2 as a function of the number of participants for Au + Au at 200 AGeV for different combinations of the strong coupling α_s and the critical energy density ε_c. See [7] for more information. Right panel: gluonic R_{AA} at midrapidity ($y \in [-0.5, 0.5]$) as extracted from simulations for central Au + Au collisions at 200 AGeV. For comparison the result from Wicks *et al.* [19] for the gluonic contribution to R_{AA} and experimental results from PHENIX [23] for π^0 and STAR [10] for charged hadrons are shown.

In addition, very exciting jet-associated particle correlations have been observed [13], which might be the result of a conical emission of propagating shock waves in form of Mach Cones induced by highly-energetic partons traversing the expanding medium [14]. Furthermore, heavy quarks are interesting for the investigation of the early stage of the QGP. Due to their large mass, initially produced heavy quarks, can cover—depending on their production point—a long distance through the QGP. Interactions on this way and subsequent modifications on heavy-quark distributions can reveal valuable information about the properties of the medium.

A large class of phenomena in heavy-ion collisions can be investigated within the framework of the kinetic transport theory. Among others, the kinetic transport model BAMPS (Boltzmann Approach to Multiparton Scatterings) [9] was developed to describe the early QGP of a HIC. Using BAMPS early thermalization of gluons within $\tau < 1\,\mathrm{fm}/c$ was demonstrated in Au + Au collisions at $\sqrt{s_{NN}} = 200\,\mathrm{GeV}$ employing Glauber initial conditions and the coupling constant $a_s = 0.3$. In addition to the elastic pQCD $gg \leftrightarrow gg$ processes, pQCD-inspired bremsstrahlung $gg \leftrightarrow ggg$ was included. This was shown to be essential for the achievment of local thermal equilibrium at that short time scale. The fast thermalization happens also in a similar way using a Color Glass Condensate as inital conditions [15].

BAMPS has been applied to simulate elliptic flow and jet quenching at RHIC energies [16] for the first time using a consistent and fully pQCD-based microscopic transport model to approach both key observables on the partonic level within a common setup. The left panel of fig. 1 shows that the medium simulated in the parton cascade BAMPS exhibits a sizable degree of elliptic flow in agreement with experimental findings at RHIC as established in [6, 7].

The extraction of the shear viscosity over entropy density ratio η/s has confirmed the essential importance of inelastic processes. Within the present description bremsstrahlung and back-reaction processes lower the shear viscosity to entropy density ratio significantly by a factor of 7, compared to the ratio when only elastic collisions are considered [17, 18]. For $a_s = 0.3$ one finds $\eta/s = 0.13$, where for $a_s = 0.6$ the values matches the lower bound of $\eta/s = 1/4\pi$ from the AdS/CFT conjecture.
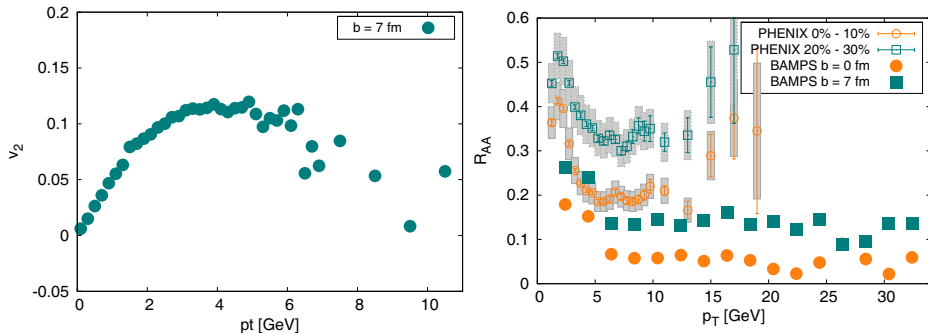
Fig. 2. – Left panel: Elliptic flow v_2 for gluons in simulated $Au + Au$ collisions at $200\,A\mathrm{GeV}$ with $b = 7\,\mathrm{fm}$. $\varepsilon_c = 0.6\,\mathrm{GeV/fm^3}$. Right panel: Gluonic R_{AA} as extracted from BAMPS simulations for $b = 0\,\mathrm{fm}$ and $b = 7\,\mathrm{fm}$, $\varepsilon_c = 1.0\,\mathrm{GeV/fm^3}$. For comparison experimental results from PHENIX [23] for π^0 are shown for central $(0–10)\%$ and off-central $(20–30)\%$ collisions.

In this paper we demonstrate the description of different phenomena in relativistic HIC using the relativistic pQCD-based on-shell parton transport model BAMPS. Due to the large momentum scales involved the energy loss of partonic jets can be treated in terms of perturbative QCD (pQCD) and most theoretical schemes attribute the main contribution to partonic energy loss to radiative processes [19]. In addition, the possible propagation of Mach Cones in the QGP induced by such highly energetic partons can be studied. Considering the earlier work investigating the effects of dissipation on relativistic shock waves [20-22] we demonstrate the transition of Mach Cones from ideal to the viscous one. It is a major challenge to combine jet physics, on the one hand, and bulk evolution, on the other hand within a common framework. In the end, the heavy quark production at RHIC and the Large Hadron Collider (LHC) during the evolution of the QGP is studied.

2. – Jet Quenching in Au + Au collisions at 200 AGeV

For simulations of Jet Quenching in heavy-ion collisions the initial gluon distributions are sampled according to a mini-jet model with a lower momentum cut-off $p_0 = 1.4\,\mathrm{GeV}$ and a K-factor of 2. The test particle method [9] is employed to ensure sufficient statistics. Quarks are discarded after sampling the initial parton distribution since currently a purely gluonic medium is considered. To model the freeze out of the simulated fireball, free streaming is applied to regions where the local energy density has dropped below a critical energy density ε_c ($\varepsilon_c = 1.0\,\mathrm{GeV/fm^3}$ unless otherwise noted).

The right panel of fig. 1 shows the gluonic R_{AA} simulated in BAMPS for central, $b = 0\,\mathrm{fm}$, collisions. It is roughly constant at $R_{AA}^{\mathrm{gluons}} \approx 0.053$ and in reasonable agreement with analytic results for the gluonic contribution to the nuclear modification factor R_{AA} [19], though the suppression of gluon jets in BAMPS appears to be slightly stronger. We expect improved agreement in future studies when employing a carefully averaged $\langle b \rangle$ that will be better suited for comparison to experimental data than the strict $b = 0\,\mathrm{fm}$ case.

We have computed the gluonic R_{AA} for non-central $Au + Au$ collisions at the RHIC energy of $\sqrt{s} = 200\,A\mathrm{GeV}$ with a fixed impact parameter $b = 7\,\mathrm{fm}$ (fig. 2), which roughly corresponds to $(20–30)\%$ experimental centrality. A comparison in terms of the magnitude of the jet suppression for $b = 7\,\mathrm{fm}$ is difficult since there are no published analytic

results available to compare to. Taking the ratio of the $b = 7$ fm to the $b = 0$ fm results as a rough guess indicates that the decrease in quenching is more pronounced in BAMPS compared to experimental data. The ratio of the nuclear modification factor between central (0–10)% and more peripheral (20–30)% collisions is $R_{AA}|_{0\%-10\%}/R_{AA}|_{20\%-30\%} \approx 0.6$ for the experimental data, while for the BAMPS results $R_{AA}|_{b=0\,\mathrm{fm}}/R_{AA}|_{b=7\,\mathrm{fm}} \approx 0.4$. However, the issue of detailed quantitative comparison needs to be re-investigated once light quarks and a fragmentation scheme are included into the simulations.

To complement the investigations of R_{AA} at a non-zero impact parameter $b = 7$ GeV, we have computed the elliptic flow parameter v_2 for gluons at the same impact parameter and extended the range in transverse momentum up to roughly $p_T \approx 10$ GeV, see left panel of fig. 2. For this a critical energy density $\varepsilon_c = 0.6$ GeV/fm^3 has been used, in order to be comparable to previous calculations of the elliptic flow within BAMPS. The v_2 of high-p_T gluons is at first rising with p_T, but from $p_T \approx 4$ to 5 GeV on, it begins to slightly decreases again. This behavior is in good qualitative agreement with recent RHIC data [24] that for charged hadrons shows v_2 to be rising up to $v_2 \approx 0.15$ at $p_T \approx 3$ GeV followed by a slight decrease.

3. – Transition from ideal to dissipative Mach Cones

There is an important issue in recent studies of relativistic heavy-ion collisions (HIC) whether the small but finite viscosity allows the development of relativistic shocks in form of Mach Cones. Within the framework of BAMPS studies were finished to answer the question whether shocks can develop with finite viscosity and how this will alter such a picture [20]. Within the relativistic Riemann problem it was shown that one dimensional shocks smears out if viscosity is large [21, 22]. However, the expected viscosity in HIC seems to be small enough to allow a significant contribution of shocks in form of Mach Cones into the picture of HIC. In the following we report a very recent study.

Mach Cones, which are special phenomena of shock waves, have their origin in ideal hydrodynamics. A very weak perturbation in a perfect fluid induces sound waves which propagate with the speed of sound $c_s = \sqrt{\mathrm{d}p/\mathrm{d}e}$, where p is the pressure and e is the energy density. In the case where the perturbation with velocity v_{jet} propagates faster than the generated sound waves, the sound waves lie on a cone. Considering a gas of massless particles, where $e = 3p$ and $c_s = 1/\sqrt{3}$, then the emission angle of the Mach Cone is given by $\alpha_w = \arccos(c_s/v_{\mathrm{jet}}) = 54.73°$.

A stronger perturbation induces the propagation of shock waves exceeding the speed of sound, therefore the emission angle changes and can be approximated by $\alpha \approx \arccos(v_{\mathrm{shock}}/v_{\mathrm{jet}})$. Here

$$(1) \qquad v_{\mathrm{shock}} = \left[\frac{(p_1 - p_0)(e_0 + p_1)}{(e_1 - e_0)(e_1 + p_0)} \right]^{1/2}$$

is the velocity of the shock front, p_0 (e_0) the pressure (energy density) in the shock front region and p_1 (e_1) in the stationary medium itself. Equation (1) has the following limits: For $p_0 \gg p_1$ we obtain $v_{\mathrm{shock}} \approx 1$, whereas for a small perturbation, $p_0 \approx p_1$, we get $v_{\mathrm{shock}} \approx c_s$.

We employ the microscopic transport model BAMPS to investigate Mach Cones with different strength of dissipations in the medium using a jet moving in positive z-direction, initialized at $t = 0$ fm/c at the position $z = -0.8$ fm. The jet is treated as a massless
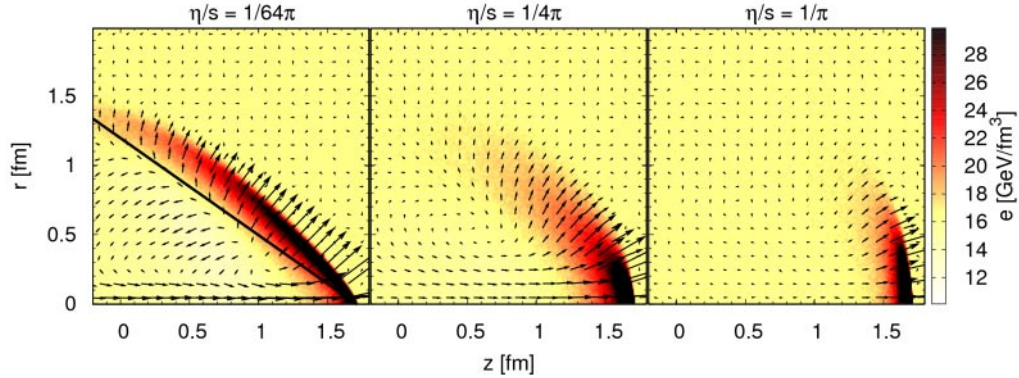
Fig. 3. – (Color online) Scenario of a massless jet with $p_z = E_{\mathrm{jet}} = 200\,\mathrm{GeV}$ which cannot be stopped by the medium—the shape of a Mach Cone shown for different viscosities of the medium, $\eta/s = 1/64\pi$ (left), $\eta/s = 1/4\pi$ (middle), $\eta/s = 1/\pi$ (right). We show the energy density plotted together with the velocity profile. Additionally, in the left panel the linear ideal Mach Cone for a very weak perturbation is shown by a solid line; its emission angle is $\alpha_w = 54.73°$.

particle with zero spatial volume and zero transverse momentum, that is, $p_z = E_{\mathrm{jet}} = 200\,\mathrm{GeV}$ and $v_{\mathrm{jet}} = 1$. The energy and momentum deposition to the medium is realized via collisions with medium particles. In this scenario we neglect the deflection of the jet and it can not be stopped by the medium; its energy and momentum is set to its initial value after every collision.

All simulations are realized within a static and uniform medium of massless Boltzmann particles and $T = 400\,\mathrm{MeV}$. For this study we consider only binary scattering processes with an isotropic cross-section among the bulk particles. To save computational runtime we reduce our problem to two dimensions. Here we choose the xz-plane and apply a periodic boundary condition in the y-direction.

In fig. 3 we demonstrate the transition from ideal Mach Cone to a highly viscous one by adjusting the shear viscosity over entropy density ratio in the medium from $\eta/s = 1/64\pi \approx 0.005$ to $1/\pi \approx 0.32$. The energy deposition of the jet is approximately $\mathrm{d}E/\mathrm{d}x = 11\text{–}14\,\mathrm{GeV/fm}$. We show a snapshot at $t = 2.5\,\mathrm{fm}/c$.

Using an unphysical small viscosity of $\eta/s = 1/64\pi$ we observe a strong collective behavior in form of a Mach Cone, as shown in the left panel of fig. 3. Due to the fact that the energy deposition is strong, the shock propagates faster than the speed of sound through the medium. For comparison, the ideal Mach Cone caused by a very weak perturbation is given by a solid line with its emission angle $\alpha_w = 54.73°$. Furthermore, a strong diffusion wake in direction of the jet, characterized by decreased energy density, and a head shock in the front are clearly visible.

If we increase the viscosity of the medium to larger values, shown in the middle and left panel of fig. 3, the typical Mach Cone structure smears out and vanishes completely. Due to stronger dissipation, the collective behavior gets weaker because of less particle interactions in the medium with a larger η/s. The results agree qualitatively with earlier studies [20,22], where a smearing-out of the shock profile is observed with higher viscosity.

In addition to the scenario of an unstoppable jet we demonstrate in fig. 4 the scenario of a massless jet with finite energy which can also be deflected. Its initial energy is set to $p_z = E_{\mathrm{jet}} = 20\,\mathrm{GeV}$, where the starting point is $z = -0.3\,\mathrm{fm}$. We show the results for different viscosities, $\eta/s \approx 0.01$ to 0.5 at $t = 5.0\,\mathrm{fm}/c$. In analogy to the results above we
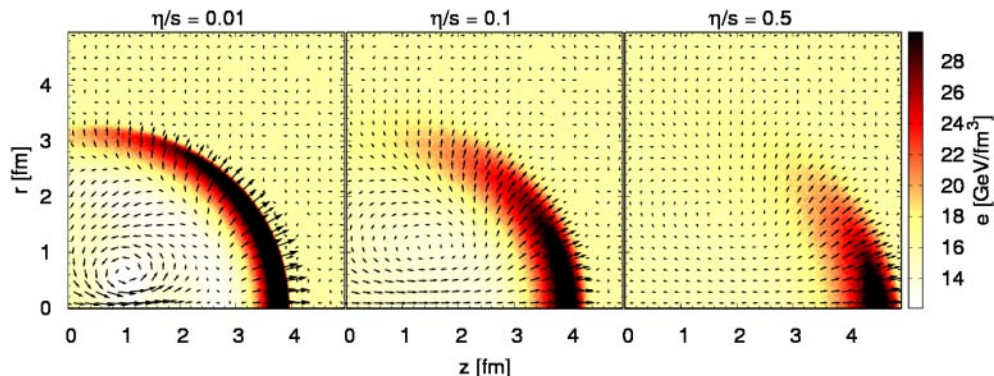
Fig. 4. – (Color online) Scenario of a deflectable jet with finite energy $p_z = E_{\text{jet}} = 20\,\text{GeV}$: Induced Mach Cone structure for different viscosities of the medium, $\eta/s = 0.01$ (left), $\eta/s = 0.1$ (middle), $\eta/s = 0.5$ (right). We show the energy density plotted together with the velocity profile.

observe a clear Mach Cone structure for small viscosities and a smearing out with larger values of η/s. Only in the ideal case a strongly curved structure in which the building up of a strong vortex is visible. The physical meaning of these phenomena and also jets with the full pQCD cascade have to be explored in future studies.

4. – Heavy quarks in BAMPS

Initial heavy quark production during hard parton interactions in nucleon-nucleon scatterings and secondary production during the evolution of the QGP are studied. We use the event generator PYTHIA [25] to determine the initial heavy quark distributions, which agree with the experimental data from PHENIX [26]. Nevertheless, these distributions have large uncertainties due to their sensitivity on the parton distribution functions in nucleons, the heavy-quark masses as well as the renormalization and factorization scales (see [27] for a detailed analysis). For the initial distribution of the gluonic medium we use three different approaches: the mini-jet model, a color glass condensate inspired model and also PYTHIA in combination with the Glauber model.

In the following we give a brief overview of our results on heavy-quark production in the QGP. More details concerning this section can be found in [27].

Secondary heavy quark production in the QGP is studied within a full BAMPS simulation of Au + Au collisions at RHIC. According to our calculations the charm quark production in the medium lies between 0.3 and 3.4 charm pairs, depending on the model of the initial gluon distribution, the charm mass and whether a $K = 2$ factor for higher-order corrections of the cross-section is employed. However, compared to the initial yield these values are of the order of a few percent for the most probable scenarios. Therefore, one can conclude that charm production at RHIC in the QGP is nearly negligible.

At LHC, however, the picture looks a bit different: Here the charm production in the QGP is a sizeable fraction of the initial yield and is even of the same order for some scenarios (with mini-jet initial conditions for gluons with a high energy density). In numbers, between 11 and 55 charm pairs are produced in the QGP.

Bottom production in the QGP, however is very small both at RHIC and LHC and can be safely neglected. As a consequence, all bottom quarks at these colliders are produced in initial hard parton scatterings.
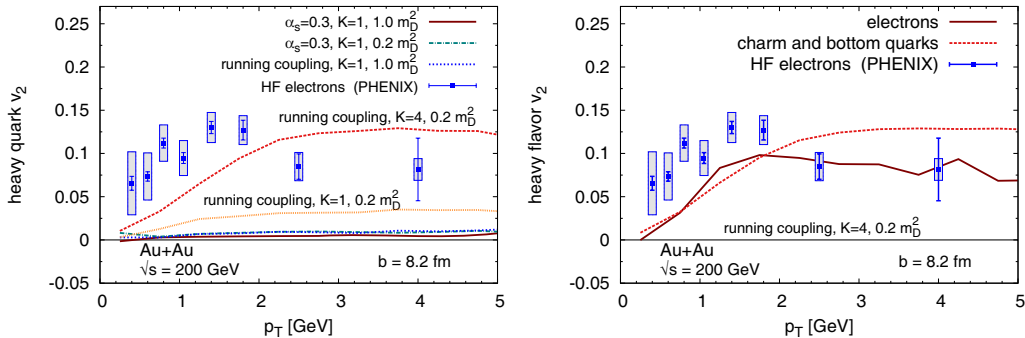
Fig. 5. – Left panel: elliptic flow v_2 of heavy quarks with pseudo-rapidity $|\eta| < 0.35$ at the end of the QGP phase for Au + Au collisions at RHIC with an impact parameter of $b = 8.2$ fm. For one curve the cross-section of $gQ \rightarrow gQ$ is multiplied with a K-factor. For comparison, data of heavy-flavor electrons [28] is also shown. In contrast to the left panel, where the theoretical curves for v_2 on the quark level are plotted, the right panel depicts the flow of heavy quarks and electrons, which stem from the decay of D and B mesons produced by fragmentation.

The elliptic flow and the nuclear modification factor

$$(2) \qquad v_2 = \left\langle \frac{p_x^2 - p_y^2}{p_T^2} \right\rangle, \qquad R_{AA} = \frac{\mathrm{d}^2 N_{AA}/\mathrm{d}p_T\,\mathrm{d}y}{N_{\mathrm{bin}}\,\mathrm{d}^2 N_{pp}/\mathrm{d}p_T\,\mathrm{d}y}$$

(p_x and p_y are the momenta in the x- and y-direction with respect to the reaction plane) of heavy quarks at mid-rapidity are observables which are experimentally measurable and reflect the coupling of heavy quarks to the medium. A large elliptic flow comparable to that of light partons indicates a strong coupling to the medium. On the other hand a small R_{AA} is a sign for a large energy loss of heavy quarks. Experimental results reveal that both quantities are on the same order as the respective values for light particles [28-30].

As we have recently shown [31] elastic scatterings of heavy quarks with the gluonic medium using a constant coupling $\alpha_s = 0.3$ and the Debye mass for screening the t channel cannot reproduce the experimentally measured elliptic flow. In order to explain the data one would need a 40–50 times larger cross-section than the leading-order one. Of course, this K-factor is too large to represent the contribution of higher-order corrections. However, as we demonstrated in ref. [32] and is shown in the following, the discrepancy with the data can be lowered—even on the leading order level—by a factor of 10 by taking the running of the coupling into account and by improving the incorporation of Debye screening. The remaining factor of 4 difference could then indeed stem from neglecting higher-order effects, which, however, must be checked in a future project.

The following calculations are done analogously to [32-34]. An effective running coupling is obtained from measurements of e^+e^- annihilation and non-strange hadronic decays of τ leptons [33, 35].

Since the t channel of the $gQ \rightarrow gQ$ cross-section is divergent it is screened with a mass proportional to the Debye mass, which is calculated by the common definition $m_D^2 = 4\pi(1 + N_f/6)\alpha_s(t)\,T^2$ with the running coupling. The proportionality factor κ of screening mass and Debye mass is mostly set to 1 in the literature without a sophisticated reason. However, one can fix this factor to $\kappa = 0.2$ by comparing the $\mathrm{d}E/\mathrm{d}x$ of the
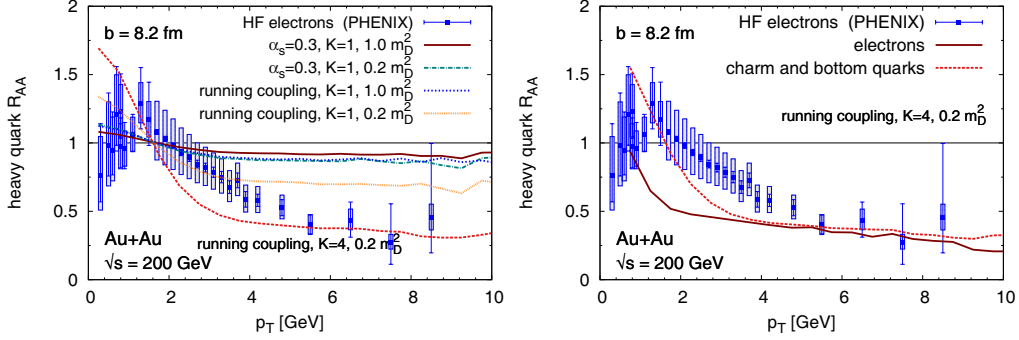
Fig. 6. – As in fig. 5, but the nuclear modification factor R_{AA} of heavy flavor is shown instead of v_2.

Born cross-section with κ to the energy loss within the hard thermal loop approach to $\kappa \approx 0.2$ [33, 34].

These improvements lead to an enhanced cross-section which also increases the elliptic flow. The left panel of fig. 5 shows v_2 as a function of the transverse momentum p_T for the leading-order cross-section without any improvements, with the running coupling, with the corrected Debye screening and with both modifications.

The elliptic flow of the latter reproduces the order of magnitude of the data, if the cross-section is multiplied with $K = 4$, which is much smaller than the previous employed $K = 40$–50 and lies in a region which could account for higher-order corrections. However, one has to check if these corrections have indeed a similar effect as a constant K-factor of 4. Therefore, the calculation of the next-to-leading order cross-section is planned for the near future and will complement $2 \leftrightarrow 3$ interactions for gluons, which are already implemented in BAMPS [9]. The shapes of the theoretical curve and of the data points are, however, slightly different. This is an effect of hadronization and decay to electrons, which is not shown in the left panel of fig. 5. If one takes those two effects into account, the agreement of the data and the theoretically curve is much better, in particular for high p_T (see right panel of fig. 5). We performed the fragmentation of charm (bottom) quarks to D (B) mesons via Peterson fragmentation [36] and used PYTHIA for the decay to electrons. At low p_T the agreement between the theoretical curve and data becomes worse, since Peterson fragmentation is not the correct model here and coalescence may play a role.

Figure 6 depicts the R_{AA} of heavy quarks, which shows for $K = 4$ the same magnitude of suppression as the data.

* * *

REFERENCES

[1] ADLER S. S. *et al.*, *Phys. Rev. Lett.*, **91** (2003) 182301.
[2] ADAMS J. *et al.*, *Phys. Rev. Lett.*, **92** (2004) 052302.
[3] BACK B. B. *et al.*, *Phys. Rev. C*, **72** (2005) 051901.
[4] LUZUM M. and ROMATSCHKE P., *Phys. Rev. C*, **78** (2008) 034915.
[5] SONG H. and HEINZ U. W., *J. Phys. G*, **36** (2009) 064033.
[6] XU Z., GREINER C. and STOCKER H., *Phys. Rev. Lett.*, **101** (2008) 082302.
[7] XU Z. and GREINER C., *Phys. Rev. C*, **79** (2009) 014904.
[8] KOVTUN P., SON D. T. and STARINETS A. O., *Phys. Rev. Lett.*, **94** (2005) 111601.
[9] XU Z. and GREINER C., *Phys. Rev. C*, **71** (2005) 064901.
[10] ADAMS J. *et al.*, *Phys. Rev. Lett.*, **91** (2003) 172302.
[11] ADLER C. *et al.*, *Phys. Rev. Lett.*, **89** (2002) 202301.
[12] ADCOX K. *et al.*, *Phys. Rev. Lett.*, **88** (2002) 022301.
[13] WANG F., *J. Phys. G*, **30** (2004) S1299.
[14] STOECKER H., *Nucl. Phys. A*, **750** (2005) 121.
[15] EL A., XU Z. and GREINER C., *Nucl. Phys. A*, **806** (2008) 287.
[16] FOCHLER O., XU Z. and GREINER C., *Phys. Rev. Lett.*, **102** (2009) 202301.
[17] XU Z. and GREINER C., *Phys. Rev. Lett.*, **100** (2008) 172301.
[18] EL A., MURONGA A., XU Z. and GREINER C., *Phys. Rev. C*, **79** (2009) 044914.
[19] WICKS S., HOROWITZ W., DJORDJEVIC M. and GYULASSY M., *Nucl. Phys. A*, **784** (2007) 426.
[20] BOURAS I. *et al.*, *Phys. Rev. Lett.*, **103** (2009) 032301.
[21] BOURAS I. *et al.*, *Nucl. Phys. A*, **830** (2009) 741c.
[22] BOURAS I. *et al.*, *Phys. Rev. C*, **82** (2010) 024910.
[23] ADARE A. *et al.*, *Phys. Rev. Lett.*, **101** (2008) 232301.
[24] ABELEV B. I. *et al.*, *Phys. Rev. C*, **77** (2008) 054901.
[25] SJOSTRAND T., MRENNA S. and SKANDS P., *JHEP*, **05** (2006) 026.
[26] ADARE A. *et al.*, *Phys. Rev. Lett.*, **97** (2006) 252002.
[27] UPHOFF J., FOCHLER O., XU Z. and GREINER C., *Phys. Rev. C*, **82** (2010) 044906.
[28] ADARE A. *et al.*, arXiv:1005.1627 [nucl-ex] (2010).
[29] ABELEV B. I. *et al.*, *Phys. Rev. Lett.*, **98** (2007) 192301.
[30] ADARE A. *et al.*, *Phys. Rev. Lett.*, **98** (2007) 172301.
[31] UPHOFF J., FOCHLER O., XU Z. and GREINER C., *J. Phys. Conf. Ser.*, **230** (2010) 012004.
[32] UPHOFF J., FOCHLER O., XU Z. and GREINER C., arXiv:1008.1995 [hep-ph] (2010).
[33] GOSSIAUX P. B. and AICHELIN J., *Phys. Rev. C*, **78** (2008) 014904.
[34] PESHIER A., arXiv:0801.0595 [hep-ph] (2008).
[35] DOKSHITZER Y. L., MARCHESINI G. and WEBBER B. R., *Nucl. Phys. B*, **469** (1996) 93.
[36] PETERSON C., SCHLATTER D., SCHMITT I. and ZERWAS P. M., *Phys. Rev. D*, **27** (1983) 105.